Experimental Neurology 362 (2023) 114344

Contents lists available at ScienceDirect

Experimental Neurology

journal homepage: www.elsevier.com/locate/yexnr

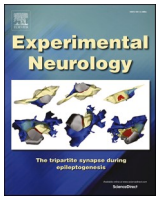

Research paper

Brain region-specific myelinogenesis is not directly linked to amyloid-β in APP/PS1 transgenic mice

Shuang-Ling Wu [a,b,1], Bin Yu [b,c,1], Yong-Jie Cheng [b,d], Shu-Yu Ren [b], Fei Wang [b], Lan Xiao [b,c], Jing-Fei Chen [b,*], Feng Mei [a,b,*]

[a] School of Medicine, Chongqing University, Chongqing 400030, China
[b] Brain and Intelligence Research Key Laboratory of Chongqing Education Commission, Department of Histology and Embryology, Third Military Medical University (Army Medical University), Chongqing 400038, China
[c] Department of Neurosurgery, 2nd Affiliated Hospital, Third Military Medical University (Army Medical University), Chongqing 400038, China
[d] Department of Neurosurgery, 1st Affiliated Hospital, Third Military Medical University (Army Medical University), Chongqing 400038, China

ARTICLE INFO

Keywords:
OPC
Oligodendroglia
Myelination
Oligodendrocyte
Demyelination

ABSTRACT

Alzheimer's disease (AD) is characterized by aggregating amyloid beta-protein (Aβ). Recent evidence has shown that insufficient myelinogenesis contributes to AD-related functional deficits. However, it remains unclear whether Aβ, in either plaque or soluble form, could alter myelinogenesis in AD brains. By cell-lineage tracing and labeling, we found both myelinogenesis and Aβ deposits displayed a region-specific pattern in the 13-month-old APP/PS1 transgenic mouse brains. Aβ plaques cause focal demyelination, but only about 15% Aβ plaques are closely associated with newly formed myelin in the APP/PS1 brains. Further, the Aβ plaque total area and the amount of new myelin are not linearly correlated across different cortical regions, suggesting that Aβ plaques induce demyelination but may not exclusively trigger remyelination. To understand the role of soluble Aβ in regulating myelinogenesis, we chose to observe the visual system, wherein soluble Aβ is detectable but without the presence of Aβ plaques in the APP/PS1 retina, optic nerve, and optic tract. Interestingly, newly-formed myelin density was not significantly altered in the APP/PS1 optic nerves and optic tracts as compared to the wildtype controls, suggesting soluble Aβ probably does not change myelinogenesis. Further, treatment of purified oligodendrocyte precursor cells (OPCs) with soluble Aβ (oligomers) for 48 h did not change the cell densities of MBP positive cells and PDGFRα positive OPCs *in vitro*. Consistently, injection of soluble Aβ into the lateral ventricles did not alter myelinogenesis in the corpus callosum of NG2-CreErt; Tau-mGFP mice significantly. Together, these findings indicate that the region-dependent myelinogenesis in AD brains is not directly linked to Aβ, but rather probably a synergic result in adapting to AD pathology.

1. Introduction

Oligodendroglial cells and myelin undergo dynamic changes in Alzheimer's disease (AD) brains (Ettle et al., 2016; Chen et al., 2021a; Chen et al., 2022). Recent evidence has shown that increased oligodendrocyte precursor cell (OPC) proliferation and differentiation during the onset and progression of the disease (Behrendt et al., 2013; Ferreira et al., 2020). Remarkably, the newly generated oligodendrocytes (OLs) and myelin sheaths in the AD mouse brains may represent a regenerative mechanism against functional declines (Ferreira et al., 2020; Chen et al., 2021a). Enhancing myelinogenesis in the AD mouse model by using either a transgenic or pharmaceutical approach can significantly rescue AD-related memory deficits and hippocampal dysfunctions (Chen et al., 2021a; McNamara and Miron, 2021; Otto, 2021; Xu et al., 2021). These findings underscore the importance of oligodendroglial differentiation and myelination in the AD brains, but the mechanisms that drive myelinogenesis remain to be elusive.

Amyloid-β (Aβ) is a hallmark of AD pathology. The amyloid cascade hypothesis proposes that Aβ accumulation is a predominant reason that causes AD-related pathogenesis and functional deficits (Hardy and

* Corresponding authors at: Brain and Intelligence Research Key Laboratory of Chongqing Education Commission, Department of Histology and Embryology, Third Military Medical University (Army Medical University), Chongqing 400038, China.
E-mail addresses: chenjingfei11@hotmail.com (J.-F. Chen), meif@tmmu.edu.cn (F. Mei).
[1] These authors have contributed equally to this work.

https://doi.org/10.1016/j.expneurol.2023.114344
Received 31 July 2022; Received in revised form 23 January 2023; Accepted 29 January 2023
Available online 2 February 2023

Higgins, 1992; Evin and Weidemann, 2002). Soluble Aβ (oligomers), such as the 42 amino acid form of amyloid β ($Aβ_{1–42}$), is elevated in the AD brain, bloodstream, cerebrospinal fluid (CSF), and aqueous humor before the onset of disease (Gyure et al., 2001; Georganopoulou et al., 2005; Lesné et al., 2013; Esparza et al., 2016). Studies have shown that soluble Aβ can pass blood brain barrier freely, and the increased level of soluble Aβ is considered as an early sign of AD (Niwa et al., 2000; Herzig et al., 2006; Jack Jr. et al., 2013). During disease progression, Aβ in the AD brain gradually aggregates as the forms of fibrils and senile plaques that continuously release soluble Aβ (Cruz et al., 1997). Numerous studies have shown that either soluble or plaque Aβ is neurotoxic and displays multiple detrimental effects on brain integrity, such as disrupting synaptic connections, activating microglial cells and astrocytes. Multiple lines of evidence have shown that Aβ is closely related to the changes of myelin and oligodendroglial cells in AD brains. For example, Aβ plaques cause focal demyelination lesions, but it is unknown yet whether the demyelinating insults can initiate a regenerative response (Mitew et al., 2010). Several studies have examined the effects of Aβ oligomers on oligodendroglial differentiation and survival *in vitro* but yielded incompletely consistent results (Xu et al., 2001; Horiuchi et al., 2012; Quintela-López et al., 2019). Therefore, it remains undefined howdoes Aβ change myelinogenesis in the AD brains.

Here, by using NG2-CreErt; Tau-mGFP mouse line to label newly-generated myelin sheaths in APP/PS1 mice, we reported that myelinogenesis and Aβ plaques in the APP/PS1 mice are brain-region dependent but not linearly correlated in the 13-month-old APP/PS1 brains after induction at the age of 6 months. Only about 15% of Aβ plaques were closely co-localized with newly generated myelin. To understand if soluble Aβ (Aβ oligomers) could change oligodendroglia differentiation, we examined the optic nerves and optic tracts wherein soluble Aβ but not Aβ plaques were detectable. Interestingly, myelinogenesis was not significantly altered in the optic nerve and optic tract, suggesting soluble Aβ may not change oligodendrocyte myelination. To examine this hypothesis, we treated purified OPCs with soluble $Aβ_{1–42}$, and the exposure to Aβ did not significantly alter the density of PDGFRα positive OPCs, O4 positive pre-oligodendrocytes and MBP positive OLs *in vitro*. Consistently, injection of Aβ oligomers into the lateral ventricles did not change the number of new myelin sheaths in the wildtype mouse brains. Together, our results indicate that Aβ is not directly linked to oligodendroglial differentiation and myelination.

2. Materials and methods

2.1. Animals

The C57BL/6 wild-type mice were purchased from the animal breeding center of Third Military Medical University. The NG2-CreERT line (Catalog #008538), the Tau-mGFP line (Catalog# 021162) and the mT/mG line (The Jackson Laboratory, Cat: 007676) were all purchased from Jackson Laboratory and were crossed to obtain NG2-CreERT; Tau-mGFP and NG2-CreERT; mT/mG mice. Then the APP/PS1 line (APPswe/PSEN1dE9, The Jackson Laboratory, Catalog# 034832) was crossed with the NG2-CreERT; Tau-mGFP line to generate APP/PS1; NG2-CreERT; Tau-mGFP and NG2-CreERT; Tau-mGFP mice as previously described (Wang et al., 2020; Chen et al., 2021a). PCR analysis of toe genomic DNA was used to distinguish different genotypes of all mouse lines with the respective primers. Male and female mice were used for all experiments, since there is no apparent gender bias in myelinogenesis. All animals in this study were cared for in accordance with an approved protocol from the Laboratory Animal Welfare and Ethics Committee of the Third Military Medical University (SYKX2017–0056).

2.2. Administration of tamoxifen

Tamoxifen (Sigma-Aldrich, Cat: T5648) was dissolved in corn oil at a concentration of 30 mg/ml. APP/PS1; NG2-CreERT; Tau-mGFP and NG2-CreERT; Tau-mGFP mice were administrated tamoxifen solution at a dose of 100 mg/kg per day by oral gavage for four consecutive days to induce recombination.

2.3. Tissue preparation

Mice were anesthetized with 1% pentobarbital. Then the mice were flushed with 0.01 M phosphate-buffered saline (PBS), followed by 4% cold paraformaldehyde (PFA) in 0.1 M phosphate buffer (PB) transcardially. For brain and optic nerve tissue collection, brains and optic nerves were collected and post-fixed in 4% PFA in 0.1 M PB at 4 °C for 24 h, followed by dehydration in 30% sucrose in 0.01 M PBS until submerged. Brains and optic nerves were embedded in optimal cutting temperature (OCT) compound (Sakura Finetek USA.Inc., 4583, USA) and cut into 10- or 20-μm thick sections respectively by cryostat microtome (Cyrostar NX50, Thermo Fisher, USA). For retina tissue collection, eyeballs were removed and post-fixed in 4% PFA in 0.1 M PB at 4 °C for 30 min immediately. The entire retina was gently dissected from the eyecup under a dissecting microscope and fixed on ice in anhydrous methanol for 30 min.

2.4. Immunofluorescence staining

For immunofluorescence staining, floating sections and fixed coverslips were washed with 0.01 M PBS, blocked with 5% bovine serum albumin (BSA, Solarbio Science & Technology Co., Ltd., A8010, Beijing) and 0.5% Triton X-100 for 1 h at room temperature and then sequentially incubated with primary antibodies overnight at 4 °C and the fluorescent-dye-conjugated secondary antibodies for 1 h at room temperature. Primary antibodies include: rabbit anti-NG2 (1:500, Millipore, Cat: AB5320), goat anti-PDGFRα(1:500, R&D, Cat: AF1062), mouse anti-O4 (1:500, Sigma, Cat:O7139), rat anti-MBP (1:200, Millipore, Cat: MAB386), rabbit anti-Iba1(1:500, Wako, Cat: 019–19,741), mouse anti-β-Amyloid (1–16) (1:500, Biolegend, Cat:803007), goat anti-GFAP (1:500, Abcam, Cat: ab53554), rabbit anti-ASPA(1:500, Millipore, Cat: ABN1698), rabbit anti-Ki67 (1:500, Abcam, Cat:ab15580), guinea pig anti-PLP (1:500, Asis Biofarm, Cat: OB-PGP028–01). Appropriate Alexa Fluor-conjugated secondary antibodies were used (1:1000, Life Technologies). The nuclei were counterstained with DAPI at room temperature.

2.5. Terminal deoxynucleotidyl transferase (TdT) dUTP Nick-End Labeling (TUNEL) assay

The TUNEL assay kit (Roche, Cat:NO12156792910) was performed according to the manufacturer's instructions. Briefly, the coverslips were washed three times with 0.01 M PBS after being fixed by 4% paraformaldehyde. Then adherent cells were incubated in permeabilization solution (0.1% Triton X-100 in 0.1% sodium citrate) for 2 min on ice. Enzyme solution and label solution were mixed in a ratio of 1:50 to obtain TUNEL reaction mixture. Incubating coverslips with TUNEL reaction mixture for 1 h at 37 °C in the dark. After washed with PBS, the nuclei were counterstained with DAPI at room temperature.

2.6. Enzyme-linked immunosorbent assay (ELISA)for $Aβ_{1–42}$

15-month-old APP/PS1 mice were anesthetized with 1% pentobarbital, followed by an initial flush with 0.01 M PBS. Hippocampus, optic nerve and retina were removed from mice brain and lysed by 0.1 M PBS separately. The supernatant obtained by centrifugation of the lysates (5000 x*g* for 5 min) was used for subsequent experiments. The protein concentration was determined by BCA Assay Kit (Beyotime, Cat: P0010S). All sample were 40-fold diluted, then the ELISA kit (Cloud-Clone Crop, Cat: CEA946Hu) was performed according to the manufacturer's instructions.

2.7. Primary OPC culture

Immunopanning purification of OPCs was performed as previously described (Lee et al., 2013; Mei et al., 2014). Briefly, OPCs were separated from 6 to 7 postnatal mouse cortex. Panning dishes were incubated with secondary and primary antibodies sequentially. After rinsing and incubating at room temperature with primary antibodies for Ran-2, GalC, and PDGFRα (1:500, R&D, AF1062), mouse brain cerebral hemispheres were diced and dissociated using papain at 37 °C for 75 min. After trituration, cells were resuspended in a panning buffer and then incubated at room temperature sequentially on three immunopanning dishes: Ran-2 and GalC were used for negative selection before positive selection with goat anti-PDGFRα. The isolated OPCs were then cultured in DMEM (Invitrogen) medium supplemented with B27 (Invitrogen), N2 (Invitrogen), penicillin-streptomycin (Invitrogen), *N*-acetylcysteine (Sigma-Aldrich), forskolin (Sigma-Aldrich) and 25 ng/ml of PDGF-AA (proliferation medium) on poly-D-lysine-coated coverslips (12 mm) in 24-well plates for 24 h before change to the same medium with PDGF-AA omitted (differentiation medium) for 48 h.

2.8. Aβ oligomer preparation

Synthetic $A\beta_{1-42}$ and reverse $A\beta_{1-42}$ (GL Biochem Ltd., Shanghai) was prepared as established protocol (Balducci et al., 2010; Zhang et al., 2019). Briefly, $A\beta_{1-42}$ and reverse $A\beta_{1-42}$ were dissolved in 1,1,1,3,3,3-hexafluoro-2-propanol HIFP(Sigma) and aliquoted to a mass of 0.1 mg per tube. Then their solutions were vacuum dried for 1 h to obtain lyophilized Aβ peptide. Lyophilized Aβ peptide was suspended in dimethyl sulfoxide (DMSO) and incubated overnight at 4 °C. The peptide suspension was diluted with differentiation medium in the absence of PDGF-AA to achieve the desired final concentrations before treatment.

2.9. $A\beta_{1-42}$ injection

The $A\beta_{1-42}$ and reverse $A\beta_{1-42}$ oligomers were dissolved in DMSO to a concentration of 0.5 mg/ml (Kim et al., 2016). 8-month-old mice were injected with 0.5 μl using a Hamilton syringe at the speed of 0.05 μl/min into the left lateral ventricle at stereotaxic coordinates (X: 0.75; Y:-0.1; Z:-2.75, relative to Bregma). Neonatal mice were injected with 20 μl per day (0.5 mg/ml) intraperitoneally from postnatal P7 to P14 (Eisele et al., 2010).

2.10. Osmotic pump implantation

The experiment was conducted according to a described protocol (Wang et al., 2021b). Osmotic pump kit with catheters (RWD, Cat: 1002 W) was used to delivery lipids into the left lateral ventricle of 8-month-old mice. The osmotic pump was connected to a catheter, filled with 100μl Aβ oligomer (0.05 mg/ml) or DMSO, then implanted subcutaneously following the manufacturer's instructions. Brain infusion cannula, connected with the catheter was fixed on the surface of skull to reach lateral ventricle. The stereotaxic coordinates were used as previously described: X: 0.75; Y:-0.1; Z:-2.75, relative to Bregma.

2.11. Images acquisition and quantification

Fluorescent images were obtained by confocal laser-scanning microscope (Olympus, FV 3000, Shinjuku, Tokyo) or a spinning disk confocal super resolution microscope (Olympus, SpinSR10, Shinjuku, Tokyo) at appropriate excitation wavelengths. 3-D reconstruction images were created by using Imaris x64 software (Bitplane, Switzerland) (Fig. 2). To quantify Iba1, GFAP, PDGFRα, ASPA and NG2 positive cells, at least three representative fields (20×) were randomly acquired. To quantify MBP-positive areas and mGFP positive areas in mice brains, at least three representative fields were randomly acquired from each set of brain section (20×). For quantification in Fig. 2C, the area of single senile plaque is the Aβ + area (blue), the area covered by the cell body and process of the microglia corralling the senile plaque is the Iba1 area (red), and the distance between the boundary of the nearby area (green) and the boundary of the Iba1 area (red) is equal to the distance between the boundary of the Iba1 area (red) and the boundary of the Aβ + area (blue). For quantification in Fig. 2F, the presence of mGFP positive new myelin sheaths in the 200 μm diameter area, with the senile plaque as the center of the circle, is considered as Aβ w/ myelin. 20 myelin segments were counted as one mGFP. A circular area with a diameter of 200 μm was drawn with this as the center of the circle, and the presence or absence of Aβ in it was measured.

2.12. Statistical analysis

Data were analyzed using SPSS software. All values are presented as the mean ± standard error of the mean (SEM). One-way ANOVA followed by Tukey test was used for comparison among three groups, and two-tailed unpaired *t*-test was used for comparison among two groups. Chi-square test was used for correlation analysis. All statistical methods, significance analyses, exact n values and other relevant information for data comparison are described in the figure legends. Significance was reported as $^{*}p < 0.05$, $^{**}p < 0.01$ or $^{***}p < 0.0001$.

3. Results

3.1. Region-dependent myelinogenesis in the APP/PS1 mouse brains

Recent studies have shown that OPC proliferation and differentiation are both elevated in the AD mouse models (Behrendt et al., 2013; Chen et al., 2021a). To characterize the pattern of myelinogenesis in AD, we crossed the APP/PS1 transgenic mouse with the NG2-CreERT; Tau-mGFP mouse line. Upon induction, the recombination occurs in the NG2 positive cells (OPCs and pericytes). The membrane-bound GFP (mGFP) is selectively expressed in myelinating OLs, as it is under the control of the Tau promoter and the Tau expression is very low in OPCs and pericytes (Young et al., 2013; Wang et al., 2020). In support with this notion, our results indicated that the mGFP positive structures are exclusively co-colocalized with the PLP positive myelin sheaths but not with the NG2 positive OPCs and immature OLs (Supplemental Fig. 1A). After being treated with tamoxifen at the age of 7 months, a large amount of newly generated OLs and associated myelin sheaths (mGFP positive) can be visualized in the NG2-CreERT; Tau-mGFP at the age of 13 months (Fig. 1A). The newly generated myelin sheaths displayed a region-dependent pattern (Fig. 1B-D). The mGFP positive new myelin was significantly increased in the APP/PS1 motor cortex, sensory cortex, and hippocampus as compared to the wildtype controls over the 6-month window (Fig. 1B-D). In contrast, the new myelin was not significantly altered in the auditory cortex and significantly decreased in the piriform cortex (Fig. 1B-D). To exclude the possibility that the brain region-dependent change of myelinogenesis is due to variable recombination efficiency in OPCs, we used the NG2-CreERT; mTomato/mGFP mice, in which the mGFP expression can be visualized in OPCs upon induction (Supplemental Fig. 1). We calculate the ratio of mGFP and NG2 double positive cells in different cortical regions (Supplemental Fig. 1B). Our results indicated that about 85% NG2 positive OPCs co-expressed mGFP throughout all the cortex regions (Supplemental Fig. 1B), indicating consistent recombination efficiency driven by NG2-CreERT. Since OPC density is almost unaltered in AD brains, we speculated that OPCs may proliferate more quickly to replace the differentiated OPCs (Chen et al., 2021a). By immunostaining for Ki67, we found that about 1–3% of PDGFRα+ positive cells co-express Ki67 in the 7-month old AD and wildtype mouse brains (Supplemental Fig. 2A). As expected, the rate of proliferative OPCs was significantly increased in the sensory cortex and hippocampus, the brain regions with enhanced myelinogenesis, as compared to the age-matched 7-month-old wildtype mice (Supplemental Fig. 2A). While the proliferative OPC density was

not significantly changed in the auditory or piriform cortex (Supplemental Fig. 2A). These results support the notion that OPCs increase proliferation in adapting to the enhanced myelinogenesis in the AD brains. The OPC differentiation is greatly inhibited in aged mouse brains (Wang et al., 2020). Consistently, we found the Ki67 positive cell density was significantly decreased in the 13-month old AD and wildtype brains as compared to 7-month old controls respectively (Supplemental Fig. 2B). In addition, we found neither the PDGFRα+ OPC density nor the proliferative rate of OPCs (PDGFRα+/Ki67+ cells) was significantly changed in the sensory and piriform cortex of 13-month old AD brains (Supplemental Fig. 2C, D), though the two brain regions displayed opposite degrees of myelinogenesis in the 7 + 6 month NG2-CreERT; Tau-mGFP AD brains (Fig. 1). This is probably due to an extremely low rate of OPC proliferation in the aged brains (Supplemental Fig. 2B). These findings indicated the region-dependent change of new myelin generation in the APP/PS1 mouse brains attributes largely to the altered OPC proliferation and differentiation.

3.2. Absence of new myelin and OPCs within the core of Aβ deposits

Previous studies have shown that Aβ deposits are one hallmark of AD-related pathological changes and also display a region-dependent

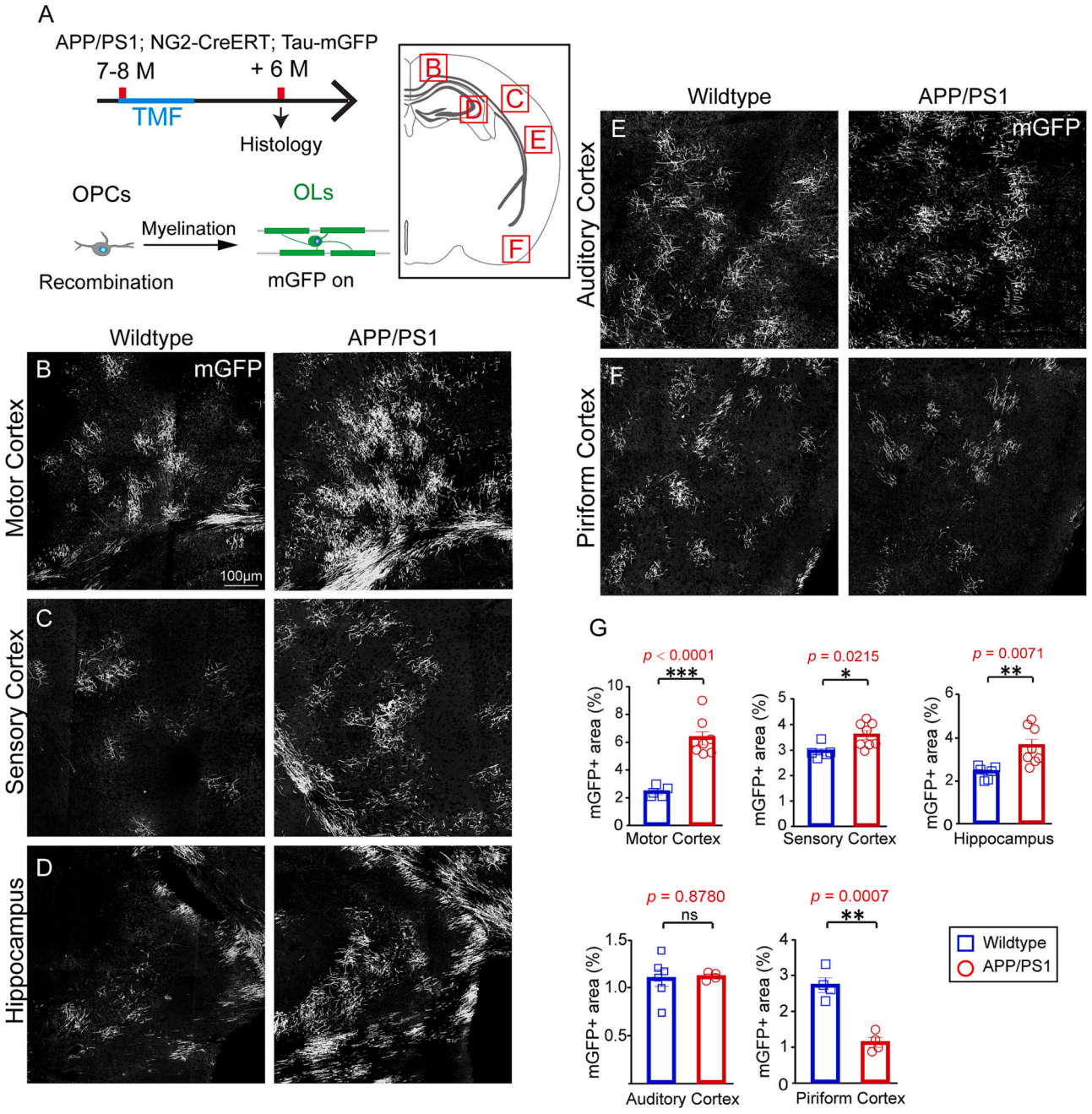

Fig. 1. Region-specific myelinogenesis in the APP/PS1 mouse brains.
(A) Schematic illustration showing the time course for tamoxifen induction and histology in the APP/PS1; NG2-CreERT; Tau-mGFP mice.
(B—D) Confocal images of mGFP-positive myelin (gray) in the motor cortex (B), sensory cortex (C), hippocampus (D) of APP/PS1 mice and age-matched controls (NG2-CreERT; Tau-mGFP). Scale bars, 100 μm.
(*E*-G) Quantification of mGFP-positive new myelin in the motor cortex, sensory cortex, hippocampus, auditory cortex and piriform cortex. $n = 5$–7 brains for each group; two-tailed unpaired *t*-tests were used. Error bars indicate mean ± SEM. $^{*}p < 0.05$, $^{**}p < 0.01$, and $^{***}p < 0.0001$. ns, not significant.

pattern (Chen et al., 2021a). In principle, Aβ plaques are more frequently detected in the cortex, hippocampus, and corpus callosum, where newly formed myelin density was also significantly increased (Fig. 1). It has been well documented that Aβ plaques cause focal demyelination in the AD brains (Brun and Englund, 1986; Mitew et al., 2010; Migliaccio et al., 2012). Similarly, we found myelin basic protein (MBP) expression was exclusively diminished in the places where Aβ plaques were detected (Fig. 2A). As a reparative mechanism, adult OPCs are capable of sensing the demyelination lesions, migrating, proliferating and eventually differentiating into mature OLs in demyelination lesions (Mei et al., 2016a; Mei et al., 2016b). Noticeably, Aβ plaques were surrounded by Iba1 positive microglial cells with an amoeboid morphology with branched processes reaching towards the Aβ plaques in the APP/PS1 cortex (Fig. 2B). To define the Aβ plaque-associated myelin kinetics, we thus calculated new myelin densities in three different regions: (1) within Aβ plaques; (2) with activated microglial; (3) the nearby region without corralling microglia and Aβ (Fig. 2C). It is evident that very few mGFP new myelin was seen within the Aβ plaques where demyelination occurs (Fig. 2). Three-dimension (3D) reconstruction assay further confirmed that new myelin sheaths were almost absent within Aβ plaques (Fig. 2C), suggesting that new myelin cannot be generated within the Aβ plaques after demyelination. Noticeably, the number of new myelin sheaths generated in the Iba1 positive area was not significantly different from the nearby area, suggesting activated microglia does not inhibit myelinogenesis (Fig. 2C).

Regarding the absence of new myelin within the Aβ plaques, we next sought to understand if this is due to OPC changes. We did immunostaining for NG2 (OPCs) and Aβ plaques. We detected very few OPC cell bodies within the Aβ plaques while the NG2 positive OPCs nearby reached out the processes towards Aβ plaques (Fig. 2D). The 3D reconstruction clearly revealed very few OPCs were present within the core of Aβ plaque (Fig. 2D), suggesting OPCs probably cannot survive or repopulate within the Aβ plaques. These results indicate that Aβ plaques induce focal demyelination and inhibits myelinogenesis owing to, at least partially, the failure of OPC repopulation.

3.3. *Aβ deposits are not specifically correlated with myelinogenesis*

If the demyelination can trigger endogenous remyelination, it sounds reasonable that newly-formed myelin sheaths prefer to localize closely to Aβ plaques. We next wanted to know if the region-dependent myelinogenesis is related to the distribution of Aβ deposits in the AD mice at the age of 13 months (Fig. 2E). We chose to analyze the correlation between myelin generation and Aβ deposition by calculating the total areas of mGFP positive new myelin and Aβ deposits in different cortical regions (Fig. 2E). We plotted the total area of mGFP positive new myelin (X-axis) of a given cortex region and the corresponding total Aβ plaque area (Y-axis) in the coordinate (Fig. 2E). We expected to see more new myelin sheaths in the brain regions with more abundant Aβ deposits, given that myelin regeneration is an intrinsic response to demyelination. Unexpectedly, our results indicated that the amount of mGFP positive new myelin is not linearly related to the total areas or numbers of Aβ deposits across different cortical regions (Fig. 2E). For example, the total amount of Aβ plaques was high in the auditory cortex but very few newly generated myelin was spotted. It seems that the amount of myelinogenesis is not directly related to Aβ plaques but dependent on the brain regions in the AD mouse. Next, we wanted to know the percentage of Aβ plaques that are closely associated with (surrounded by) new myelin sheaths. Interestingly, only about 15% percent of Aβ plaques were surrounded by new myelin. On the other hand, about only 10% of new myelin is co-existing with Aβ plaques (Fig. 2F). Since the Aβ plaque begins to emerge at the age of 4–5 months, we examined the relationship between myelinogenesis and Aβ deposition in 5-month-old APP/PS1; NG2-CreERT; Tau-mGFP mice (Supplemental Fig. 2E, F). Similarly, only about 11% percent of Aβ plaques were surrounded by new myelin 1 month after induction at the age of 4 months. These results suggest that Aβ deposition and myelinogenesis are not spatiotemporally correlated, implying Aβ plaques cause demyelination and seemingly do not increase myelinogenesis in the AD mouse brain. Since Aβ plaques activate microglia, we next wanted to examine if this region-specific myelinogenesis is related to the function of microglia somehow. We calculated the Iba1 positive microglia with myelin debris (MBP+) engulfed in the regions displaying different degrees of myelinogensis (Supplemental Fig. 2G). And our results indicated that the amount of microglia with engulfed myelin debris was not significantly different between the motor cortex and the piriform cortex (Supplemental Fig. 2G). These results suggest that the brain-region changes of myelin may not be related to the debris clearance functions by microglia.

3.4. *Absence of Aβ deposits in the visual pathway*

The Aβ plaques are considered as a source of soluble Aβ oligomers and the concentration of which is higher in the places that are closer to the cores in distance (Hyman et al., 1993; Cruz et al., 1997; Koffie et al., 2009). Indeed, soluble Aβ (oligomers) is detectable in the brains at the early stage of AD, raising the possibility of soluble Aβ in regulating myelinogenesis. Admittedly, it is difficult to model an *in vivo* condition with solely the presence of soluble Aβ but not Aβ aggregation. We and others noticed the Aβ plaques distributed in a region-dependent manner and were absent in some brain regions. Previous studies have shown that Aβ plaque was not detected in the APP/PS1 retina (Sadun and Bassi, 1990; Chidlow et al., 2017). We examined Aβ plaques in the visual system of 15-month old APP/PS1 mice. Our results indicated that Aβ deposits are extensively detected in the visual cortex but undetectable in the APP/PS1 optic nerve, and optic tract (Fig. 3B-H). It is evident that the Aβ plaques in the APP/PS1 visual cortex were surrounded by activated microglial cells and astrocytes (Fig. 3B). While, the cell density of neither Iba1 positive microglia nor the GFAP positive astrocytes was significantly changed in the retina and optic nerves in the 15-month APP/PS1 mice (Fig. 3D-H), indicating that retinal neurons and their axonal projections are exposed to soluble Aβ but not Aβ plaques (Sadun and Bassi, 1990; Chidlow et al., 2017). In support of this notion, a number of studies have shown that Aβ oligomers ($A\beta_{1-42}$) are detectable in brain, CSF, and aqueous humor from the early stages of AD (Gong et al., 2003; Georganopoulou et al., 2005; Lesné et al., 2013; Kwak et al., 2020). We also detected soluble $A\beta_{1-42}$ in the hippocampus, optic nerve and retina of 15-month-old APP/PS1 mice by ELISA (Fig. 4A), confirming that the optic nerve and tract are ideal for examining whether soluble Aβ can alter myelinogenesis *in vivo*.

3.5. *Unaltered myelinogenesis in the optic nerve and optic tract*

We next examined new myelin generation by calculating the mGFP positive new myelin in the 13-month APP/PS1; NG2-CreErt; Tau-mGFP optic nerve and optic tract after induction at the age of 7 months (Fig. 4B). Newly generated myelin sheaths can be visualized in the optic nerves and optic tracts. Quantitative results indicated the amount of new myelin generation in the AD optic nerve and tracts were not significantly different from the age-matched wildtype controls (Fig. 4C, D). We did immunostaining for aspartoacylase (ASPA), a marker for labeling mature OL cell bodies. Quantitative results indicated the amount newly generated OL (ASPA/mGFP double-positive cell) were not significantly changed in optic tracts of APP/PS1 mice and age-matched wildtype controls (Fig. 4E). These results suggest that soluble Aβ exposure may not change myelinogenesis in the APP/PS1 CNS.

3.6. *Soluble Aβ does not change OPC differentiation in vitro and in vivo*

To further confirm the effect of soluble Aβ (oligomers) on oligodendroglial differentiation and myelination, we next utilized OPC cultures to examine if soluble $A\beta_{1-42}$ oligomers can change OPC differentiation *in vitro*. The mouse OPCs were purified from the P6–7

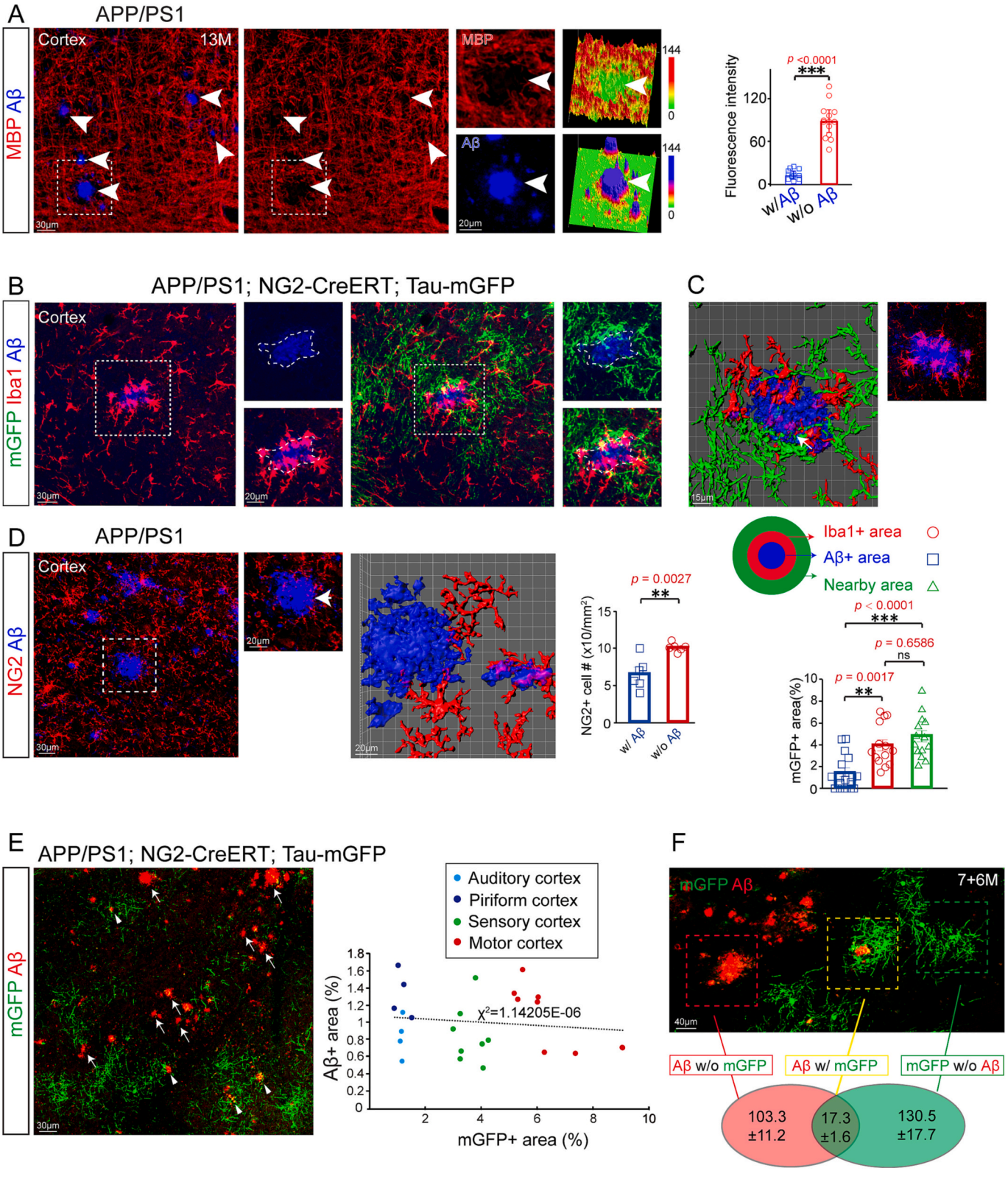

(caption on next page)

Fig. 2. New myelin distribution around Aβ deposits.
(A) Representative images and quantification of MBP (red) and Aβ (blue, arrows) in the 13-month APP/PS1 brains and magnified and heatmap images showing the MBP and Aβ gray value in the left subpanel. $n = 12–13$ Aβ plaques from 3 mice. Scale bars, 30 μm (left panels) and 20 μm (right panels).
(B) Representative images showing mGFP (green), Iba1(red) and Aβ (blue) in the 13-month cortex of APP/PS1; NG2-CreERT; Tau-mGFP and magnified images showing the Aβ plaques (outlined area), Iba1 positive microglial cells and mGFP-positive myelin. Scale bars, 30 μm (left panels) and 20 μm (right panels).
(C) Three-dimension reconstruction of Aβ (blue), Iba1+ microglia (red) and mGFP positive new myelin (green). Arrow indicating the myelin sheath within the Aβ plaque. Quantification of mGFP+ myelin in Aβ + area (blue), Iba1 area (red) and nearby area (green). One-way ANOVA followed by Bonferroni's test was used for comparison among three groups. $n = 17–18$ Aβ plaques from 3 mice; Scale bars,15 μm; Two-tailed unpaired t-tests were used. Error bars indicate mean ± SEM. $^{**}p < 0.01$, and $^{***}p < 0.0001$.
(D) Confocal (left and middle images) and three-dimensional reconstruction photos (right image) of NG2-positive OPCs (red) and Aβ (blue) in the cortex of APP/PS1 transgenic mice. Arrows indicating the Aβ plaques. Quantification of NG2-positive OPCs in the cortex and magnified images. $n = 4–5$ biologically independent mice for each group; Scale bars,30 μm(left panels) and 20 μm (right panels). Two-tailed unpaired *t*-tests were used. Error bars indicate mean ± SEM. $^{*}p < 0.05$, $^{**}p < 0.01$, and $^{***}p < 0.0001$.
(E) Representative image showing mGFP positive new myelin (green) and Aβ (red) in the cortex of APP/PS1; NG2-CreERT; Tau-mGFP. Graph showing a correlation between the areas of new myelin (X-axis) and Aβ deposition (Y-axis). Scale bars,30 μm. n = 4–8 biologically independent mice for each group; two-tailed unpaired *t*-tests were used. Error bars indicate mean ± SEM. Chi-square test was used for correlation analysis.
(F) Confocal images showing Aβ plaques without (Aβ w/o mGFP) or with (Aβ w/ myelin) mGFP positive new myelin, and mGFP positive myelin without Aβ (mGFP w/o Aβ). The average numbers of Aβ plaques were collected from 3 biologically independent mice. Scale bars,40 μm. (For interpretation of the references to colour in this figure legend, the reader is referred to the web version of this article.)

mouse cortex by immunopanning and seeded on coverslips coated with L-polylysine. 48 h after seeding, the OPCs were treated with soluble $Aβ_{1–42}$ oligomers, reverse $Aβ_{1–42}$ oligomers at 1 μM, or vehicle for 48 h before being collected for immunostaining. We calculated the total cell number (DAPI positive), OPCs (PDGFRα positive), and OLs (MBP positive) on the coverslips (Fig. 5A). Our results indicated that the overall cell density and the PDGFRα or MBP positive cell density were not significantly altered after exposure to soluble Aβ oligomers or reverse Aβ oligomers as compared to the controls (Fig. 5B). The MBP+ cells displayed similar morphology and complexity among the three groups (Fig. 5B). To understand if there are changes of oligodendroglial cells at the intermediate stage of differentiation or undergoing apoptosis, we examined premature OLs by immunostaining for O4 and apoptotic cells by TdT-mediated dUTP nick end labeling (TUNEL) respectively. Neither O4 positive cell density nor TUNEL positive cell density was significantly changed by Aβ oligomers treatment (Fig. 5C, D). These results indicated that Aβ oligomers at 1 μM do not significantly alter the survival rate of OLs nor change OPC differentiation *in vitro*. To understand if Aβ oligomers can change the differentiation and myelination of neonatal OPCs *in vivo*, we chose to inject Aβ oligomers intraperitoneal into P7 neonatal mice for 7 days (Supplemental Fig. 3A). Our results indicated that the exposure to Aβ oligomers did not change MBP positive myelin areas in the P14 brain (Supplemental Fig. 3B, C).

To examine whether soluble Aβ can change OPC differentiation and myelination *in vivo*, we induced recombination one week prior to injection soluble $Aβ_{1–42}$ into the lateral ventricles of the 8-month-old NG2-CreERT; Tau-mGFP brains (Fig. 6). We chose to observed the new myelin formation in the cortex and corpus callosum, given active myelination in these two regions and that closely localized to ventricles. After one dose of injection into the ventricle, the mice were sacrificed two weeks after the injection (Fig. 6A), since newly formed myelin is detectable one week after induction(Chen et al., 2021b). The mGFP positive new myelin was observed in all the brain regions in the vehicle brains and we calculated the mGFP positive new myelin area and the average length of myelin sheaths in the cortex and corpus callosum (Fig. 6B, C). Our results indicated that neither the new myelin density nor the average myelin length of each OL was significantly altered in the Aβ-injected brains as compared to the vehicle controls (Fig. 6B, C). Because brain soluble Aβ can flows out and be cleared physiologically(Eisele et al., 2010), we next implanted a osmotic pump to consecutively deliver Aβ oligomers into lateral ventricles for 2 weeks, and examined if consistent exposure to Aβ oligomers can change myelinogenesis *in vivo*. Consistently, the mGFP positive new myelin area in the cortex and corpus callosum were not significantly changed between vehicle and Aβ oligomers groups (Fig. 6 D, E). These findings, combined with the *in vitro* result, suggest that soluble Aβ oligomers may not alter myelinogenesis significantly in the wildtype mouse brains.

4. Discussion

Our results indicated that myelinogenesis is brain-region dependent in the AD mouse brains. Aβ plaques cause focal demyelination but are unlikely trigger robust myelinogenesis. In addition, soluble Aβ does not change oligodendroglial differentiation and myelination both *in vitro* and *in vivo*. These results demonstrate that the myelinogenesis is not directly coupled with Aβ, but rather a synergic result in responsible to AD pathological changes.

It has been well documented that Aβ plaques induce focal demyelination (Mitew et al., 2010). As an intrinsic mechanism to repair the demyelination lesions, adult OPCs are capable of repopulating within the demyelination lesions and differentiating into mature OLs (Kang et al., 2010; Mei et al., 2014). In the brain regions with increased myelinogenesis, it is evident that OPCs proliferate at a higher rate to maintain the population. However, we found OPCs are almost devoid within the core of Aβ plaques, suggesting the absence of OPCs and senescence-like changes may be the reason that dampens new myelin generation (Zhang et al., 2019). The reasons that oligodendroglial cells cannot survive within the Aβ plaques remain unclear yet. One possibility is that Aβ plaques are cytotoxic and may cause cell death (Xu et al., 2001; Bero et al., 2012). A recent study has revealed that the turnover of myelin-related protein is impaired in the APP knock-in cortex and hippocampus regions, suggesting compromised protein homeostasis may be involved in AD related myelin changes (Hark et al., 2021). Additionally, the activated microglial cells may induce focal inflammation and cause cell apoptosis or senescent changes by producing oxidative factors and cytokines (Hansen et al., 2018). Microglia engulf myelin debris and can change the OPC differentiation. Our results suggest the myelin debris engulfing function is not altered in different brain regions. Nevertheless, it remains possible that the heterogeneity of microglia in AD brains may contribute to myelin dynamics (Masuda et al., 2020; Wang, 2021). Besides that, new myelin deposition is largely dependent on axon availability and acceptance. The AD-related pathology changes of axons may determine, at least partially, the place and amount of newly-formed myelin sheaths (Jawhar et al., 2012; Alobuia et al., 2013). These results demonstrate that Aβ plaques are a detrimental environment against oligodendroglial survival and new myelin generation, and the myelinogenesis in AD brain can be influenced by various factors.

Of note, new myelin sheaths can be generated around a portion of Aβ plaques (Chen et al., 2021a). It has been shown that the concentration of soluble Aβ is higher in the area that is closer to the Aβ plaques. Besides, myelinogenesis in the area without Aβ plaques is also greatly enhanced, raising the possibility that soluble Aβ probably could change oligodendroglial differentiation and myelination. Previous studies have shown that soluble Aβ may inhibit membrane sheet formation of OL or promote oligoendroglial differentiation and myelination by using purified OPCs

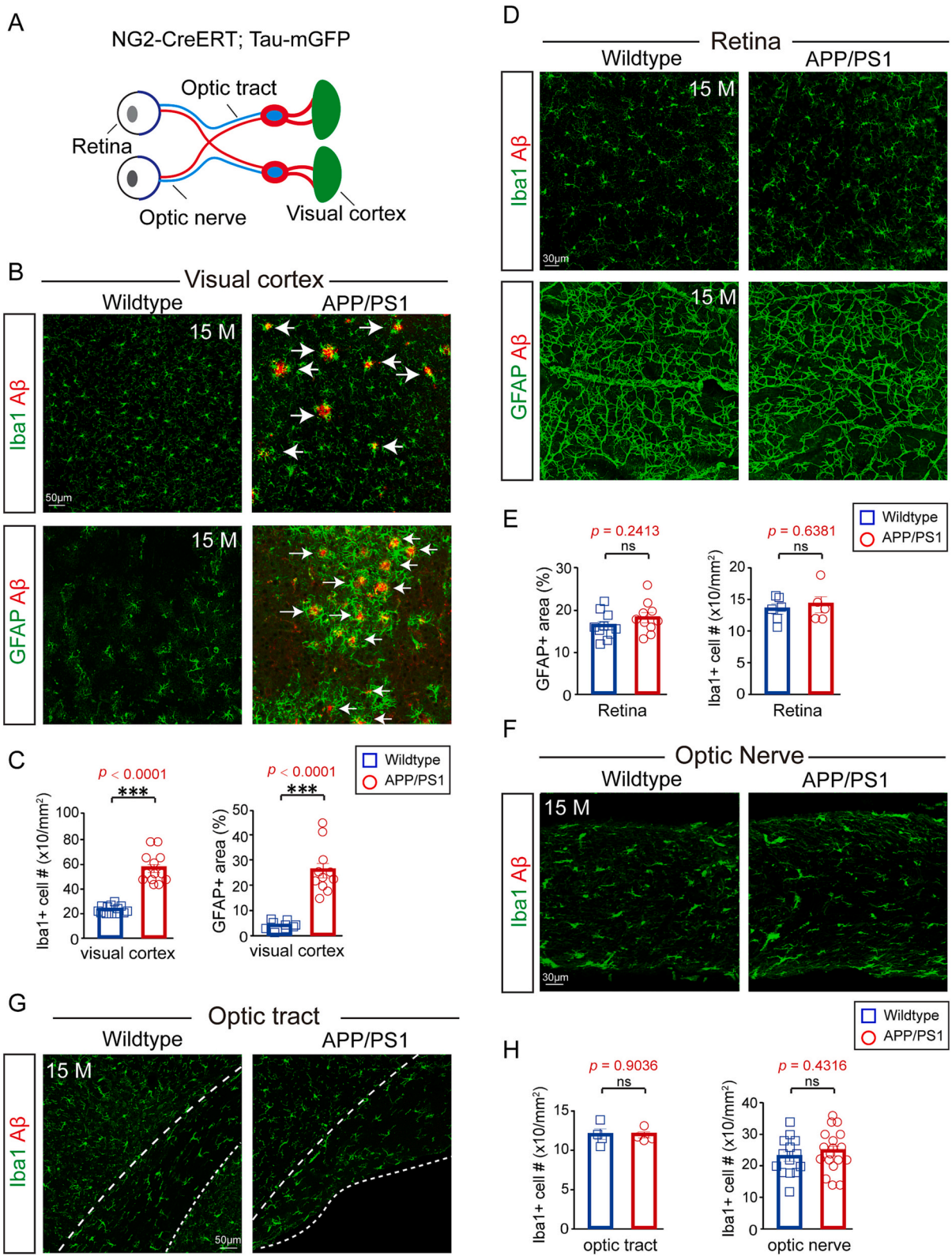

Fig. 3. Aβ deposits and glia activation in the visual pathway.
(A) Schematic illustration showing visual pathway including the retina, optic nerve, optic tract and visual cortex.
(B-E) Representative images and quantification of Iba1 (B, C), GFAP (D, E) and Aβ in the visual cortex and retina of 15-month-old APP/PS1 transgenic mice and age-matched wild-type controls. Scale bars, 50 μm (B) and 30 μm(D). n = 12 brain sections (C), or 5–10 retina samples (D) from 3 biologically independent mice for each group.
(F—H) Representative images and quantification of Iba1(green) and Aβ(red) in the optic nerve and optic tract of 15-month-old APP/PS1 transgenic mice and age-matched wild-type controls. n = 4 biologically independent mice (H left graph), or 16 optical nerve sections from 3 mice (H right graph) for each group.
Two-tailed unpaired *t*-tests were used. Scale bars, 50 μm (G) and 30 μm (F). Error bars indicate mean ± SEM. ***p < 0.0001. ns, not significant. (For interpretation of the references to colour in this figure legend, the reader is referred to the web version of this article.)

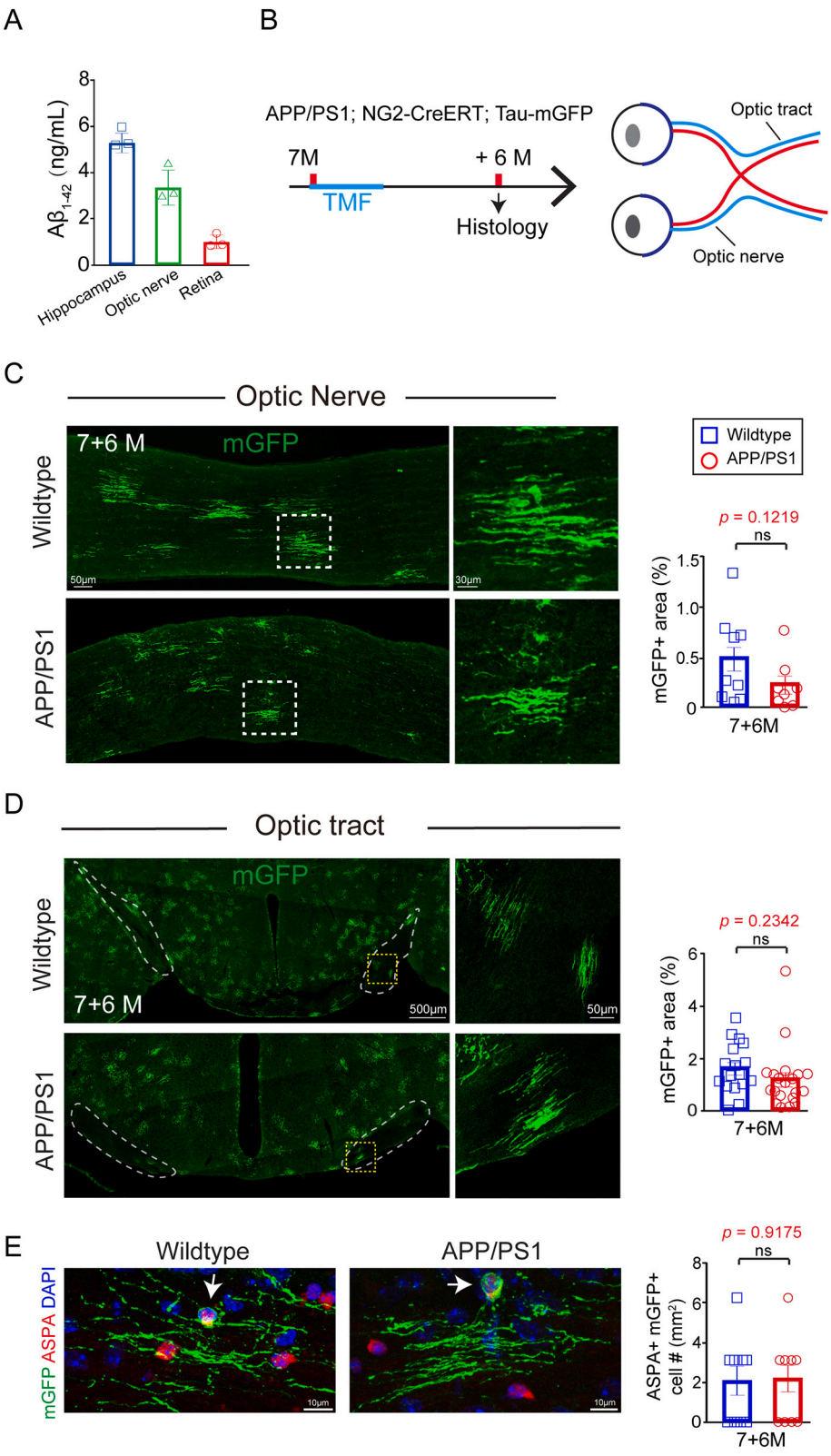

Fig. 4. Myelinogenesis in APP/PS1 visual pathway.
(A) Concentration of soluble $A\beta_{1-42}$ detected by ELISA assay kit. $n = 3$ biologically independent mice for each group.
(B) Schematic illustration displaying the time course for tamoxifen induction and histology in the APP/PS1; NG2-CreERT; Tau-mGFP mice.
(C—D) Representative images and quantification of mGFP-positive myelin in the optic nerve and optic tract of APP/PS1 mice and littermate controls. Scale bars, 50 μm (C, left panels) , 30 μm (C, right panels), 500 μm (D, left panels) and 50 μm (D, right panels). $n = 7–10$ optic nerves (C), or 16 optic tracts (D) from 5 mice for each group; two-tailed unpaired *t*-tests were used.
(E) Representative images and quantification of mGFP (green), ASPA(red) and DAPI(blue) in the optic tract of 15-month-old APP/PS1 transgenic mice and age-matched wild-type controls.
$n = 10–16$ optic tracts from 5 mice; two-tailed unpaired *t*-tests were used. Scale bars, 10 μm. Error bars indicate mean ± SEM. ns, not significant.

from rat optic nerve and brains (Horiuchi et al., 2012; Quintela-López et al., 2019). Interestingly, our results indicated that exposure to soluble Aβ oligomers for 48 h did not change the differentiation or survival of oligodendroglia in the cultures of purified OPCs from mouse cortex. The discrepancy of how does soluble Aβ change oligodendroglia differentiation in cultures remains unclear from the current data set. It is possible that the differences of OPCs in either species or brain regions may contribute to the inconsistence. We used mouse OPCs purified from P6–7 cortex to examine the effect of soluble Aβ on OPC differentiation. In line with this finding, injection of soluble Aβ to P7 neonatal mouse pups does not alter myelination at the age of P14. These results suggest that soluble Aβ may not alter OPC differentiation *in vitro and in vivo*. Injection of

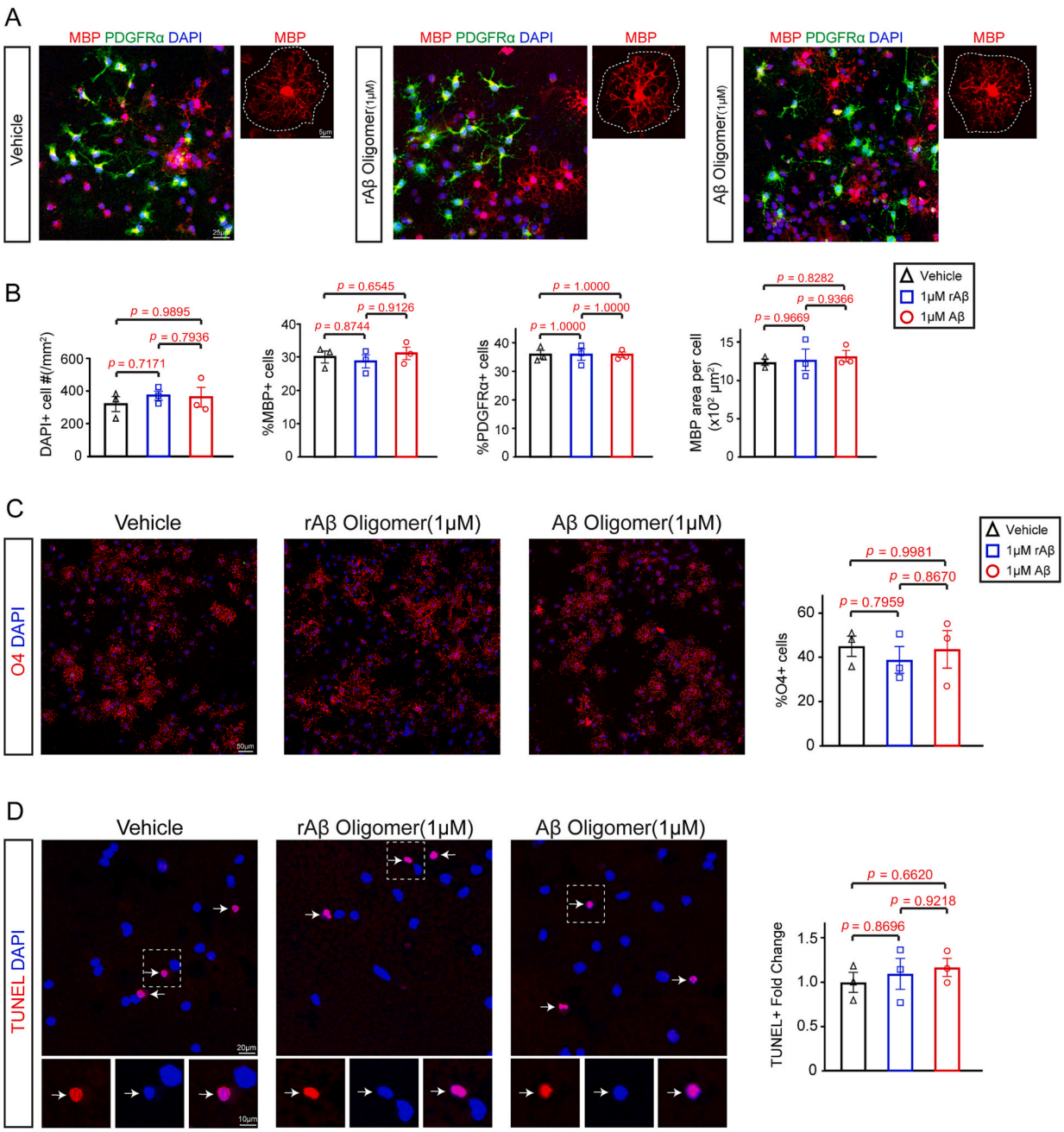

Fig. 5. Effect of soluble Aβ on purified OPC cultures.
(A) Purified OPC culture were treated with vehicle, reverse Aβ oligomer (rAβ) or Aβ oligomer (Aβ) for 48h and immunostained for MBP (red), PDGFRα (green). Coverslips were counterstained for DAPI (blue). Scale bars, 100 μm. High magnification images with superimposed dotted line showing single MBP+ cell morphology (right panel). Scale bars, 5 μm.
(B) Cell density of DAPI positive cells, MBP positive cells and PDGFRα positive cells and quantification of average area of MBP+ cells. n = 3–9 coverslips; One-way ANOVA followed by Tukey's test was used for comparison among three groups.
(C) Representative images and quantification of O4 positive cells. n = 3–9 coverslips; Scale bars, 50 μm. One-way ANOVA followed by Tukey's test was used for comparison among three groups.
(D) Representative images and quantification of TUNEL positive cells. White arrow indicates single TUNEL+ cell. High magnification images of single TUNEL+ cell (Bottom). n = 3–9 coverslips; One-way ANOVA followed by Tukey's test was used for comparison among three groups. Error bars indicate mean ± SEM. ns, not significant. (For interpretation of the references to colour in this figure legend, the reader is referred to the web version of this article.)

soluble Aβ oligomers into the lateral ventricle nor exposure to soluble Aβ during early development did not change the myelinogenesis in adult or neonatal brains. These results collectively showed that short-term or consecutive exposure to soluble Aβ oligomers does not change oligodendroglial differentiation and myelination *in vitro and in vivo*.

To examine the effect of long-term exposure to soluble Aβ oligomers, we observed the myelinogenesis in the visual system, specifically the retina ganglion cells and their axonal projections into brains. We chose to observe visual system for three reasons: (1) soluble Aβ is can be detected in the AD brains, bloodstream, CSF, and aqueous humor and the concentration of soluble Aβ oligomers in the aqueous humor is positively related to the bloodstream and CSF (Esparza et al., 2016; Kwak et al., 2020); (2) only soluble Aβ but not Aβ plaques were detected in retina and optic nerves, excluding the effects of Aβ plaques (Sadun

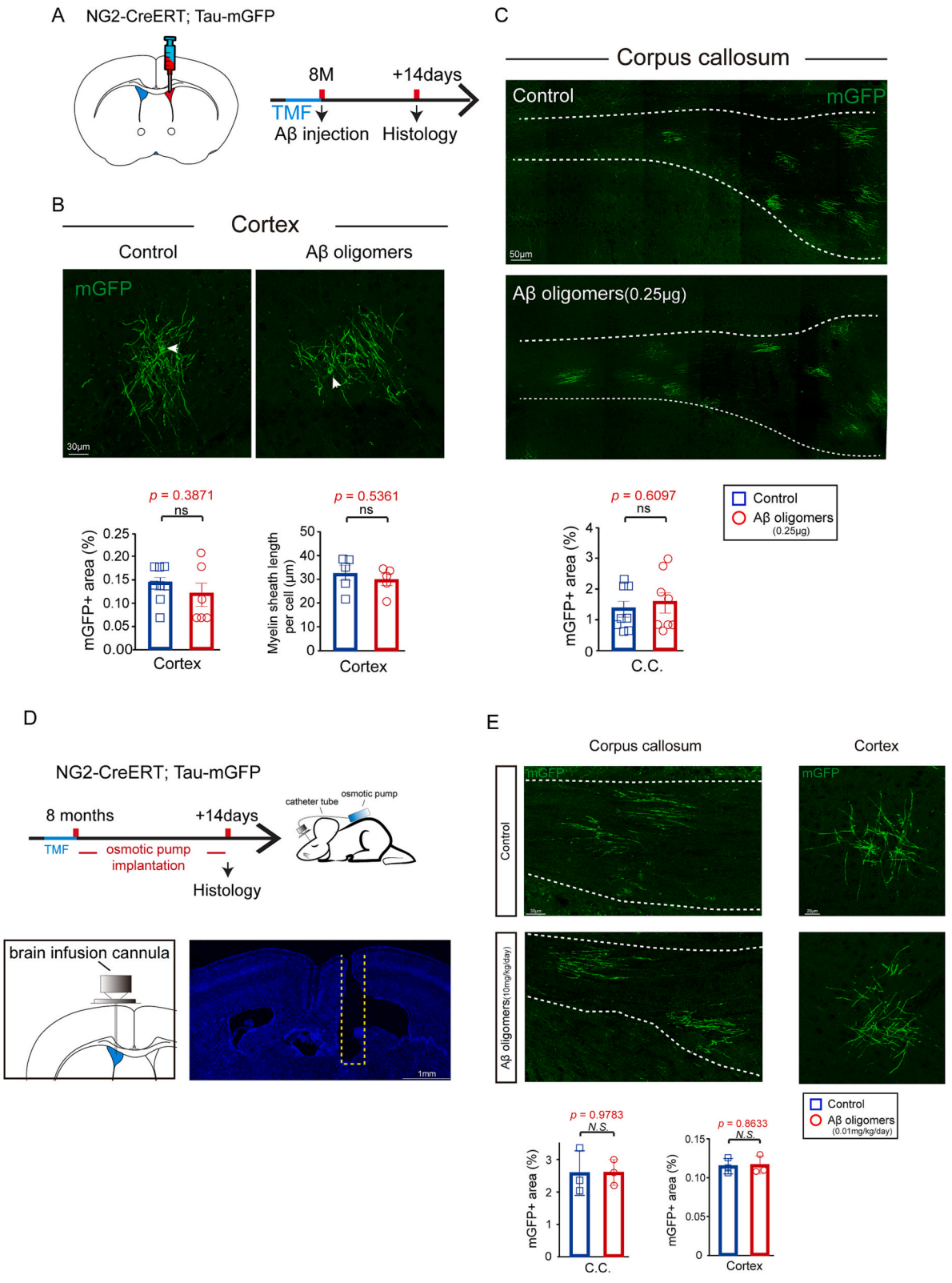

Fig. 6. Effect of soluble Aβ on myelinogenesis in the NG2-CreERT; Tau-mGFP brains.
(A) Schematic diagram displaying the time course of tamoxifen (TMF) treatment, Aβ injection and histology.
(B—C) Representative images and quantification of mGFP-positive myelin in the cortex and corpus callosum of Aβ oligomer and control mice. And the quantification of average length of myelin sheaths in the cortex. Scale bars,30 μm(B) and 50 μm(C). n = 5–9 biologically independent mice for each group; two-tailed unpaired *t*-tests were used. Error bars indicate mean ± SEM. ns, not significant.
(D) Schematic illustration showing the time course for osmotic pump implantation and histology of the NG2-CreERT; Tau-mGFP mice.
(E) Representative images and quantification of mGFP-positive myelin in the cortex and corpus callosum of Aβ oligomer and control mice. Scale bars, 30 μm (left) and 20 μm (right). n = 3 biologically independent mice for each group; two-tailed unpaired t-tests were used. Error bars indicate mean ± SEM. ns, not significant.

and Bassi, 1990; Davies et al., 1995; Chidlow et al., 2017); (3) the visual system is going through a chronic AD process. In line with the *in vitro* results, we did not find a significant increase of mGFP positive new myelin in the optic nerve and optic tract, suggesting a chronic exposure of soluble Aβ does not change myelinogenesis in the AD brains. Thus, the mechanism underlying the region-dependent myelinogenesis remains unclear. There are numerous pathology changes going on in AD brain, such as neurofibrillary tangles and disrupted lipid metabolism (Bloom, 2014; Wang et al., 2021a; Blanchard et al., 2022). It is possible the region-dependent myelinogenesis is a synergic result in responding to multiple AD-related pathology changes.

Together, our results indicate that the brain-region dependent myelinogenesis in AD is not directly linked to Aβ plaques or soluble Aβ, but rather an intrinsic mechanism that responds to the complexity of AD-related pathology changes.

Supplementary data to this article can be found online at https://doi.org/10.1016/j.expneurol.2023.114344.

Funding

This work was supported by STI 2030—Major Projects (2021ZD0201702), the National Natural Science Foundation of China (82171417, 32200787), Chongqing Education Commission Fund (CXQT19009), Chongqing Outstanding Young Investigator Fund Project (cstc2019jcyjjqx0011) and School Management Foundation of Third Military Medical University (2020XQN04).

CRediT authorship contribution statement

Shuang-Ling Wu: Formal analysis, Data curation, Methodology, Resources, Writing - original draft. **Bin Yu:** Data curation, Methodology, Supervision. **Yong-Jie Cheng:** Data curation, Methodology, Formal analysis. **Shu-Yu Ren:** Data curation, Methodology, Formal analysis, Resources. **Fei Wang:** Data curation, Methodology, Formal analysis, Resources, Funding acquisition. **Lan Xiao:** Resources, Supervision, Investigation. **Jing-Fei Chen:** Conceptualization, Writing – original draft, Investigation, Writing – review & editing, Data curation. **Feng Mei:** Conceptualization, Investigation, Supervision, Funding acquisition, Resources, Project administration, Writing - review & editing.

Declaration of Competing Interest

The authors declare that they have no known competing financial interests or personal relationships that could have appeared to influence the work reported in this paper.

Data availability

Data will be made available on request.

References

Alobuia, W.M., Xia, W., Vohra, B.P., 2013. Axon degeneration is key component of neuronal death in amyloid-β toxicity. Neurochem. Int. 63 (8), 782–789. https://doi.org/10.1016/j.neuint.2013.08.013.

Balducci, C., Beeg, M., Stravalaci, M., Bastone, A., Sclip, A., Biasini, E., et al., 2010. Synthetic amyloid-beta oligomers impair long-term memory independently of cellular prion protein. Proc. Natl. Acad. Sci. U. S. A. 107 (5), 2295–2300. https://doi.org/10.1073/pnas.0911829107.

Behrendt, G., Baer, K., Buffo, A., Curtis, M.A., Faull, R.L., Rees, M.I., et al., 2013. Dynamic changes in myelin aberrations and oligodendrocyte generation in chronic amyloidosis in mice and men. Glia 61 (2), 273–286. https://doi.org/10.1002/glia.22432.

Bero, A.W., Bauer, A.Q., Stewart, F.R., White, B.R., Cirrito, J.R., Raichle, M.E., et al., 2012. Bidirectional relationship between functional connectivity and amyloid-β deposition in mouse brain. J. Neurosci. 32 (13), 4334–4340. https://doi.org/10.1523/jneurosci.5845-11.2012.

Blanchard, J.W., Akay, L.A., Davila-Velderrain, J., von Maydell, D., Mathys, H., Davidson, S.M., et al., 2022. APOE4 impairs myelination via cholesterol dysregulation in oligodendrocytes. Nature 611 (7937), 769–779. https://doi.org/10.1038/s41586-022-05439-w.

Bloom, G.S., 2014. Amyloid-β and tau: the trigger and bullet in Alzheimer disease pathogenesis. JAMA Neurol 71 (4), 505–508. https://doi.org/10.1001/jamaneurol.2013.5847.

Brun, A., Englund, E., 1986. A white matter disorder in dementia of the Alzheimer type: a pathoanatomical study. Ann. Neurol. 19 (3), 253–262. https://doi.org/10.1002/ana.410190306.

Chen, J.F., Liu, K., Hu, B., Li, R.R., Xin, W., Chen, H., et al., 2021a. Enhancing myelin renewal reverses cognitive dysfunction in a murine model of Alzheimer's disease. Neuron 109 (14). https://doi.org/10.1016/j.neuron.2021.05.012, 2292–2307 e2295.

Chen, L., Ren, S.Y., Li, R.X., Liu, K., Chen, J.F., Yang, Y.J., et al., 2021b. Chronic exposure to hypoxia inhibits Myelinogenesis and causes motor coordination deficits in adult mice. Neurosci. Bull. 37 (10), 1397–1411. https://doi.org/10.1007/s12264-021-00745-1.

Chen, J.F., Wang, F., Huang, N.X., Xiao, L., Mei, F., 2022. Oligodendrocytes and myelin: active players in neurodegenerative brains? Dev Neurobiol 82 (2), 160–174. https://doi.org/10.1002/dneu.22867.

Chidlow, G., Wood, J.P., Manavis, J., Finnie, J., Casson, R.J., 2017. Investigations into retinal pathology in the early stages of a mouse model of Alzheimer's disease. J. Alzheimers Dis. 56 (2), 655–675. https://doi.org/10.3233/jad-160823.

Cruz, L., Urbanc, B., Buldyrev, S.V., Christie, R., Gómez-Isla, T., Havlin, S., et al., 1997. Aggregation and disaggregation of senile plaques in Alzheimer disease. Proc. Natl. Acad. Sci. U. S. A. 94 (14), 7612–7616. https://doi.org/10.1073/pnas.94.14.7612.

Davies, D.C., McCoubrie, P., McDonald, B., Jobst, K.A., 1995. Myelinated axon number in the optic nerve is unaffected by Alzheimer's disease. Br. J. Ophthalmol. 79 (6), 596–600. https://doi.org/10.1136/bjo.79.6.596.

Eisele, Y.S., Obermüller, U., Heilbronner, G., Baumann, F., Kaeser, S.A., Wolburg, H., et al., 2010. Peripherally applied Abeta-containing inoculates induce cerebral beta-amyloidosis. Science 330 (6006), 980–982. https://doi.org/10.1126/science.1194516.

Esparza, T.J., Wildburger, N.C., Jiang, H., Gangolli, M., Cairns, N.J., Bateman, R.J., et al., 2016. Soluble amyloid-beta aggregates from human Alzheimer's disease brains. Sci. Rep. 6, 38187. https://doi.org/10.1038/srep38187.

Ettle, B., Schlachetzki, J.C.M., Winkler, J., 2016. Oligodendroglia and myelin in neurodegenerative diseases: more than just bystanders? Mol. Neurobiol. 53 (5), 3046–3062. https://doi.org/10.1007/s12035-015-9205-3.

Evin, G., Weidemann, A., 2002. Biogenesis and metabolism of Alzheimer's disease Abeta amyloid peptides. Peptides 23 (7), 1285–1297. https://doi.org/10.1016/s0196-9781(02)00063-3.

Ferreira, S., Pitman, K.A., Wang, S., Summers, B.S., Bye, N., Young, K.M., et al., 2020. Amyloidosis is associated with thicker myelin and increased oligodendrogenesis in the adult mouse brain. J. Neurosci. Res. 98 (10), 1905–1932. https://doi.org/10.1002/jnr.24672.

Georganopoulou, D.G., Chang, L., Nam, J.M., Thaxton, C.S., Mufson, E.J., Klein, W.L., et al., 2005. Nanoparticle-based detection in cerebral spinal fluid of a soluble pathogenic biomarker for Alzheimer's disease. Proc. Natl. Acad. Sci. U. S. A. 102 (7), 2273–2276. https://doi.org/10.1073/pnas.0409336102.

Gong, Y., Chang, L., Viola, K.L., Lacor, P.N., Lambert, M.P., Finch, C.E., et al., 2003. Alzheimer's disease-affected brain: presence of oligomeric a beta ligands (ADDLs) suggests a molecular basis for reversible memory loss. Proc. Natl. Acad. Sci. U. S. A. 100 (18), 10417–10422. https://doi.org/10.1073/pnas.1834302100.

Gyure, K.A., Durham, R., Stewart, W.F., Smialek, J.E., Troncoso, J.C., 2001. Intraneuronal abeta-amyloid precedes development of amyloid plaques in down syndrome. Arch Pathol Lab Med 125 (4), 489–492. https://doi.org/10.5858/2001-125-0489-iaapdo.

Hansen, D.V., Hanson, J.E., Sheng, M., 2018. Microglia in Alzheimer's disease. J. Cell Biol. 217 (2), 459–472. https://doi.org/10.1083/jcb.201709069.

Hardy, J.A., Higgins, G.A., 1992. Alzheimer's disease: the amyloid cascade hypothesis. Science 256 (5054), 184–185. https://doi.org/10.1126/science.1566067.

Hark, T.J., Rao, N.R., Castillon, C., Basta, T., Smukowski, S., Bao, H., et al., 2021. Pulse-chase proteomics of the app Knockin mouse models of Alzheimer's disease reveals that synaptic dysfunction originates in presynaptic terminals. Cell Syst 12 (2). https://doi.org/10.1016/j.cels.2020.11.007, 141–158.e149.

Herzig, M.C., Van Nostrand, W.E., Jucker, M., 2006. Mechanism of cerebral beta-amyloid angiopathy: murine and cellular models. Brain Pathol. 16 (1), 40–54. https://doi.org/10.1111/j.1750-3639.2006.tb00560.x.

Horiuchi, M., Maezawa, I., Itoh, A., Wakayama, K., Jin, L.W., Itoh, T., et al., 2012. Amyloid β1-42 oligomer inhibits myelin sheet formation in vitro. Neurobiol. Aging 33 (3), 499–509. https://doi.org/10.1016/j.neurobiolaging.2010.05.007.

Hyman, B.T., Marzloff, K., Arriagada, P.V., 1993. The lack of accumulation of senile plaques or amyloid burden in Alzheimer's disease suggests a dynamic balance between amyloid deposition and resolution. J. Neuropathol. Exp. Neurol. 52 (6), 594–600. https://doi.org/10.1097/00005072-199311000-00006.

Jack Jr., C.R., Knopman, D.S., Jagust, W.J., Petersen, R.C., Weiner, M.W., Aisen, P.S., et al., 2013. Tracking pathophysiological processes in Alzheimer's disease: an updated hypothetical model of dynamic biomarkers. Lancet Neurol. 12 (2), 207–216. https://doi.org/10.1016/s1474-4422(12)70291-0.

Jawhar, S., Trawicka, A., Jenneckens, C., Bayer, T.A., Wirths, O., 2012. Motor deficits, neuron loss, and reduced anxiety coinciding with axonal degeneration and intraneuronal Aβ aggregation in the 5XFAD mouse model of Alzheimer's disease. Neurobiol. Aging 33 (1). https://doi.org/10.1016/j.neurobiolaging.2010.05.027, 196.e129–140.

Kang, S.H., Fukaya, M., Yang, J.K., Rothstein, J.D., Bergles, D.E., 2010. NG2+ CNS glial progenitors remain committed to the oligodendrocyte lineage in postnatal life and

following neurodegeneration. Neuron 68 (4), 668–681. https://doi.org/10.1016/j.neuron.2010.09.009.
Kim, H.Y., Lee, D.K., Chung, B.R., Kim, H.V., Kim, Y., 2016. Intracerebroventricular injection of amyloid-β peptides in Normal mice to acutely induce Alzheimer-like cognitive deficits. J. Vis. Exp. 109 https://doi.org/10.3791/53308.
Koffie, R.M., Meyer-Luehmann, M., Hashimoto, T., Adams, K.W., Mielke, M.L., Garcia-Alloza, M., et al., 2009. Oligomeric amyloid beta associates with postsynaptic densities and correlates with excitatory synapse loss near senile plaques. Proc. Natl. Acad. Sci. U. S. A. 106 (10), 4012–4017. https://doi.org/10.1073/pnas.0811698106.
Kwak, D.E., Ko, T., Koh, H.S., Ji, Y.W., Shin, J., Kim, K., et al., 2020. Alterations of aqueous humor Aβ levels in Aβ-infused and transgenic mouse models of Alzheimer disease. PLoS One 15 (1), e0227618. https://doi.org/10.1371/journal.pone.0227618.
Lee, S., Chong, S.Y., Tuck, S.J., Corey, J.M., Chan, J.R., 2013. A rapid and reproducible assay for modeling myelination by oligodendrocytes using engineered nanofibers. Nat. Protoc. 8 (4), 771–782. https://doi.org/10.1038/nprot.2013.039.
Lesné, S.E., Sherman, M.A., Grant, M., Kuskowski, M., Schneider, J.A., Bennett, D.A., et al., 2013. Brain amyloid-β oligomers in ageing and Alzheimer's disease. Brain 136 (Pt 5), 1383–1398. https://doi.org/10.1093/brain/awt062.
Masuda, T., Sankowski, R., Staszewski, O., Prinz, M., 2020. Microglia heterogeneity in the single-cell era. Cell Rep. 30 (5), 1271–1281. https://doi.org/10.1016/j.celrep.2020.01.010.
McNamara, N.B., Miron, V.E., 2021. Replenishing our mind orchards: enhancing myelin renewal to rescue cognition in Alzheimer's disease. Neuron 109 (14), 2204–2206. https://doi.org/10.1016/j.neuron.2021.06.024.
Mei, F., Fancy, S.P.J., Shen, Y.A., Niu, J., Zhao, C., Presley, B., et al., 2014. Micropillar arrays as a high-throughput screening platform for therapeutics in multiple sclerosis. Nat. Med. 20 (8), 954–960. https://doi.org/10.1038/nm.3618.
Mei, F., Lehmann-Horn, K., Shen, Y.A., Rankin, K.A., Stebbins, K.J., Lorrain, D.S., et al., 2016a. Accelerated remyelination during inflammatory demyelination prevents axonal loss and improves functional recovery. Elife 5. https://doi.org/10.7554/eLife.18246.
Mei, F., Mayoral, S.R., Nobuta, H., Wang, F., Desponts, C., Lorrain, D.S., et al., 2016b. Identification of the kappa-opioid receptor as a therapeutic target for oligodendrocyte Remyelination. J. Neurosci. 36 (30), 7925–7935. https://doi.org/10.1523/jneurosci.1493-16.2016.
Migliaccio, R., Agosta, F., Possin, K.L., Rabinovici, G.D., Miller, B.L., Gorno-Tempini, M. L., 2012. White matter atrophy in Alzheimer's disease variants. Alzheimers Dement. 8 (5 Suppl) https://doi.org/10.1016/j.jalz.2012.04.010. S78-87.e71-72.
Mitew, S., Kirkcaldie, M.T., Halliday, G.M., Shepherd, C.E., Vickers, J.C., Dickson, T.C., 2010. Focal demyelination in Alzheimer's disease and transgenic mouse models. Acta Neuropathol. 119 (5), 567–577. https://doi.org/10.1007/s00401-010-0657-2.
Niwa, K., Carlson, G.A., Iadecola, C., 2000. Exogenous a beta1-40 reproduces cerebrovascular alterations resulting from amyloid precursor protein overexpression in mice. J. Cereb. Blood Flow Metab. 20 (12), 1659–1668. https://doi.org/10.1097/00004647-200012000-00005.
Otto, G., 2021. Myelin loss in AD. Nat. Rev. Neurosci. 22 (8), 456–457. https://doi.org/10.1038/s41583-021-00492-2.
Quintela-López, T., Ortiz-Sanz, C., Serrano-Regal, M.P., Gaminde-Blasco, A., Valero, J., Baleriola, J., et al., 2019. Aβ oligomers promote oligodendrocyte differentiation and maturation via integrin β1 and Fyn kinase signaling. Cell Death Dis. 10 (6), 445. https://doi.org/10.1038/s41419-019-1636-8.
Sadun, A.A., Bassi, C.J., 1990. Optic nerve damage in Alzheimer's disease. Ophthalmology 97 (1), 9–17. https://doi.org/10.1016/s0161-6420(90)32621-0.
Wang, H., 2021. Microglia heterogeneity in Alzheimer's disease: insights from single-cell technologies. Front Synaptic Neurosci 13, 773590. https://doi.org/10.3389/fnsyn.2021.773590.
Wang, F., Ren, S.Y., Chen, J.F., Liu, K., Li, R.X., Li, Z.F., et al., 2020. Myelin degeneration and diminished myelin renewal contribute to age-related deficits in memory. Nat. Neurosci. 23 (4), 481–486. https://doi.org/10.1038/s41593-020-0588-8.
Wang, C., Xiong, M., Gratuze, M., Bao, X., Shi, Y., Andhey, P.S., et al., 2021a. Selective removal of astrocytic APOE4 strongly protects against tau-mediated neurodegeneration and decreases synaptic phagocytosis by microglia. Neuron 109 (10), 1657–1674.e1657. https://doi.org/10.1016/j.neuron.2021.03.024.
Wang, X., Su, Y., Hu, X., Niu, J., 2021b. Osmotic pump-based drug-delivery for in vivo Remyelination research on the central nervous system. J. Vis. Exp. 178 https://doi.org/10.3791/63343.
Xu, J., Chen, S., Ahmed, S.H., Chen, H., Ku, G., Goldberg, M.P., et al., 2001. Amyloid-beta peptides are cytotoxic to oligodendrocytes. J. Neurosci. 21 (1), Rc118. https://doi.org/10.1523/JNEUROSCI.21-01-j0001.2001.
Xu, M.Y., Xu, Z.Q., Wang, Y.J., 2021. White Matter "Matters" in Alzheimer's Disease. Neurosci. Bull. https://doi.org/10.1007/s12264-021-00803-8.
Young, K.M., Psachoulia, K., Tripathi, R.B., Dunn, S.J., Cossell, L., Attwell, D., et al., 2013. Oligodendrocyte dynamics in the healthy adult CNS: evidence for myelin remodeling. Neuron 77 (5), 873–885. https://doi.org/10.1016/j.neuron.2013.01.006.
Zhang, P., Kishimoto, Y., Grammatikakis, I., Gottimukkala, K., Cutler, R.G., Zhang, S., et al., 2019. Senolytic therapy alleviates Aβ-associated oligodendrocyte progenitor cell senescence and cognitive deficits in an Alzheimer's disease model. Nat. Neurosci. 22 (5), 719–728. https://doi.org/10.1038/s41593-019-0372-9.